

Coupled Multi-Proca Vector Dark Energy

L. Gabriel Gómez¹ and Yeinzon Rodríguez^{1,2,3}

¹*Escuela de Física, Universidad Industrial de Santander,
Ciudad Universitaria, Bucaramanga 680002, Colombia*

²*Centro de Investigaciones en Ciencias Básicas y Aplicadas,
Universidad Antonio Nariño, Cra 3 Este # 47A-15, Bogotá D.C. 110231, Colombia and*

³*Simons Associate at The Abdus Salam International Centre for Theoretical Physics, Strada Costiera 11, I-34151, Trieste, Italy*

(Dated: April 15, 2020)

We study a new class of vector dark energy models where multi-Proca fields A_μ^a are coupled to cold dark matter by the term $f(X)\tilde{\mathcal{L}}_m$ where $f(X)$ is a general function of $X \equiv -\frac{1}{2}A_\mu^a A_\mu^a$ and $\tilde{\mathcal{L}}_m$ is the cold dark matter Lagrangian. From here, we derive the general covariant form of the novel interaction term sourcing the field equations. This result is quite general in the sense that encompasses Abelian and non-Abelian vector fields. In particular, we investigate the effects of this type of coupling in a simple dark energy model based on three copies of canonical Maxwell fields to realize isotropic expansion. The cosmological background dynamics of the model is examined by means of a dynamical system analysis to determine the stability of the emergent cosmological solutions. As an interesting result, we find that the coupling function leads to the existence of a novel scaling solution during the dark matter dominance. Furthermore, the critical points show an early contribution of the vector field in the form of dark radiation and a stable de Sitter-type attractor at late times mimicking dark energy. The cosmological evolution of the system as well as the aforementioned features are verified by numerical computations. Observational constraints are also discussed to put the model in a more phenomenological context in the light of future observations.

I. INTRODUCTION

Our current understanding of the universe is based on the standard model of cosmology, in short Λ CDM (Λ Cold Dark Matter) [1]. Under this realization, the universe is experiencing today an accelerated expansion due to a constant energy density characterized by some repulsive pressure and attributed to the cosmological constant [2–4]. Despite its success, the model has been the subject of intense debate due to some controversies and problems when confronted with observations, such as the cosmological constant problem [5, 6] and the inference of some spatial curvature suggested by the lensing amplitude in the cosmic microwave background power spectra [7]. Likewise, recent observations of the redshift-space distortion [8] and cluster counts [9–11] have pointed out a lower rate for the cosmic growth than that predicted by the Λ CDM model.

However, perhaps one of the major concerns in the scientific community about the standard model of cosmology, among the aforementioned internal inconsistencies, is the lack of conciliation between early and late time universe measurements which has been referred to as the Hubble tension [12]. The Planck experiment infers a value $H_0 = 67.4 \pm 0.5$ km/s/Mpc at 68% C.L., assuming the standard Λ CDM model [1] while the recent value determined from the observation of long-period Cepheids in the Large Magellanic Cloud [13] is $H_0 = 74.03 \pm 1.42$ km/s/Mpc at 68% C.L., thereby putting the standard model in tension.

Three major routes have been established, among the numerous theoretical proposals (see e.g [6, 14, 15] and references therein), to reconcile such discrepancies and

other issues in the Λ CDM model. These are, modifying the geometric sector of Einstein gravity by breaking its fundamental assumptions [16, 17], including extra fields minimally coupled to gravity which leads to dynamical dark energy (DE) such as quintessence [18, 19] and k-essence [20–22], or extending gravity by building non-minimal interactions between matter and gravity¹ [23–27]. Yet, within the second possibility, interactions between dark matter and DE are allowed. This idea has been explored intensively through phenomenological interactions introduced into the conservation equations. We are not going to discuss however the vast amount of possible choices studied in the literature; instead, we refer to [28, 29] and references therein for the cosmological implications of non-trivial functional forms of couplings. It has been shown however that this artificial description introduces both inconsistencies with the covariant stress energy conservation and instabilities [30]. Hence, one must appeal for a more fundamental and robust approach to account for such a coupling within the dark sector based, for instance, on a field theoretical description. Under this perspective, several consistent approaches have been developed to build coupled dark energy models at the level of the action such as conformal/disformal transformations [31–33], scalar-fluid theories [34, 35] and the post-Friedmannian formalism [36]. Yet another possibility is to couple directly the DE field to the matter Lagrangian, i.e., at the Lagrangian level, through a coupling function as has been proposed in a pioneering work called

¹ It is important to clarify that Horndeski theories include all the generalized Jordan-Brans-Dicke type varieties, such as quintessence and k-essence [15].

coupled quintessence [37]. This type of coupling, and more general non-trivial ones, can arise naturally after an appropriate conformal transformation which relates the metric in the Jordan frame, where matter lives, and the Einstein frame, where gravity is described by general relativity [32]. No matter the underlying physical origin of the coupling, that is, whether it comes from high energy physics arguments or from another yet unknown physical reason, one can motivate the interaction with the aim of addressing some inconsistencies in the standard cosmological model with the phenomenological interest of testing their observational signatures.

It is important to mention that most of the existing (coupled) dark energy models are based on scalar fields with little or no presence of space-like vector fields. This is because, unlike time-like vector fields, space-like vector fields can generate a large amount of anisotropy which is inconsistent with observations [1]. Nevertheless, one may avoid this undesirable result either by taking a large number of random vector fields so that, on average, they lead to an isotropic universe [38] or by considering a set of three space-like vector fields of the same norm and pointing towards mutually orthogonal spatial directions, shaping what is called the cosmic triad [39]. We highlight, up to the best of our knowledge, some significant progress in the construction of coupled vector dark energy models based on space-like vector fields such as the cosmic triad cosmology [40], three-form dark energy models [41–43], extensions of the pioneering vector-like dark energy model [39] through phenomenological interactions [44, 45] and direct coupling driving anisotropic expansion [46]. It is worth mentioning that a coupled vector dark energy model has been proposed recently [47] in the context of the generalized Proca theory [48–52] with a trivial time-like vector configuration to comply with the background symmetry.

We study in this work a novel coupling between multiple vector fields and matter of the form $f(X)\tilde{\mathcal{L}}_m$, where $f(X)$ is a general function of $X \equiv -\frac{1}{2}A_\mu^a A_\mu^a$ and $\tilde{\mathcal{L}}_m$ is the matter Lagrangian, following closely the spirit of the kinetically coupled scalar dark energy scenario [53]. Our main purpose is to extend the kinetic scalar coupling to an analogous vector coupling which is fully independent of the assumed model and on the Abelian/non-Abelian nature of the vector fields. To investigate its cosmological implications, we frame this coupling into a model consisting of three copies of the standard Maxwell-theory, consistent with the isotropic background, with a specific power law form for the coupling and an exponential potential.

The content of this paper is structured as follows. We derive, in section II, the general interaction term for the proposed coupling function. In section III, we study its cosmological behaviour by a dynamical system analysis in a specific setup consisting of the cosmic triad compatible with a Friedmann-Lemaître-Robertson-Walker (FLRW) universe. We confirm the obtained qualitative features by numerically solving the cosmological evolution of the

system in section V. Finally, the discussion and perspectives of this work are presented in section IV.

II. THE MODEL

We start by writing the general \mathcal{L}_2 piece of the Lagrangian for the generalized multi-Proca theory [54, 55] that involves only gauge-invariant and spontaneous symmetry breaking quantities which are present in the Abelian and non-Abelian cases. Indeed, any function of a set of vector fields A_μ^a , their associated gauge field strength tensors $F_{\mu\nu}^a$, and their Hodge duals $\tilde{F}_{\mu\nu}^a$ belongs to \mathcal{L}_2^2 :

$$\mathcal{L}_2 \equiv f(A_\mu^a, F_{\mu\nu}^a, \tilde{F}_{\mu\nu}^a). \quad (1)$$

Thus, the action involving the Einstein-Hilbert Lagrangian \mathcal{L}_{EH} , the \mathcal{L}_2 piece, and the explicit coupling between a mass-type term $X \equiv -\frac{1}{2}A_\mu^a A_\mu^a$ of the vector fields and matter reads

$$\mathcal{S} = \int d^4x \sqrt{-g} (\mathcal{L}_{EH} + \mathcal{L}_2 + f(X)\tilde{\mathcal{L}}_m), \quad (2)$$

where g is the determinant of the metric. The novel contribution of this paper is the inclusion of the coupling function³ $f(X)$ that describes the way in which multi-Proca fields A_μ^a couple to matter. The latter, in turn, is described by the Lagrangian $\tilde{\mathcal{L}}_m(g_{\mu\nu}, \psi)$, where ψ is the matter field. In particular, we consider the action

$$\mathcal{S} = \int d^4x \sqrt{-g} \left(\frac{M_p^2}{2} R - \frac{1}{4} F_{\mu\nu}^a F_a^{\mu\nu} - V(\tilde{X}) + f(X)\tilde{\mathcal{L}}_m \right), \quad (3)$$

where M_p is the reduced Planck mass, R is the Ricci scalar, $F_{\mu\nu}^a \equiv \nabla_\mu A_\nu^a - \nabla_\nu A_\mu^a$, and V is a potential term, as in the uncoupled model [39], where we have defined the quantity $\tilde{X} \equiv A_\mu^a A_\mu^a$.

We assume for simplicity that radiation and baryons are completely uncoupled, otherwise we will have to pass to a physical frame (usually the Einstein frame where gravity is described by general relativity) through a conformal transformation [31].

On the other hand, it is interesting to note that, in contrast to phenomenological interactions, the coupling at the level of the action affects not only the continuity equations of each matter component but also the gravitational field equations. Hence, by varying the action in

² Here a labels the different vector fields and becomes a group index if there exists some internal symmetry group.

³ A similar coupling was studied in the context of the generalized Proca theory with a time-like vector field [47]. However, our approach differs from it in that we derive here the associated interacting terms.

eqn. (3) with respect to the metric, we obtain the gravitational field equations

$$\frac{M_p^2}{2} G_{\mu\nu} = T_{\mu\nu}^A + f \tilde{T}_{\mu\nu}^m + f_{,X} \tilde{\mathcal{L}}_m A_\mu^a A_{\nu a}, \quad (4)$$

where the energy-momentum tensor of the multi-Proca fields is

$$\begin{aligned} T_{\mu\nu}^A &\equiv -2 \frac{\delta \mathcal{L}_A}{\delta g^{\mu\nu}} + \mathcal{L}_A g_{\mu\nu} \\ &= F_{\mu\sigma}^a F_{a\nu}^\sigma + 2V_{,\tilde{X}} A_\mu^a A_{\nu a} - \left(\frac{1}{4} F_{\rho\sigma}^a F_a^{\rho\sigma} + V(\tilde{X}) \right) g_{\mu\nu}, \end{aligned} \quad (5)$$

\mathcal{L}_A being defined by

$$\mathcal{L}_A \equiv -\frac{1}{4} F_{\mu\nu}^a F_a^{\mu\nu} - V(\tilde{X}). \quad (6)$$

Note that we have introduced for abbreviation the definitions $f_{,X} \equiv \frac{df}{dX}$ and $V_{,\tilde{X}} \equiv \frac{dV}{d\tilde{X}}$ in the above expressions. It is convenient to redefine the matter energy-momentum tensor according to the gravitational field equations in eqn. (4) such that

$$\begin{aligned} T_{\mu\nu}^m &\equiv -2 \frac{\delta \mathcal{L}_m}{\delta g^{\mu\nu}} + \mathcal{L}_m g_{\mu\nu} \\ &= f \tilde{T}_{\mu\nu}^m + f_{,X} \tilde{\mathcal{L}}_m A_\mu^a A_{\nu a}, \end{aligned} \quad (7)$$

where we have defined for convenience $\mathcal{L}_m \equiv f \tilde{\mathcal{L}}_m$ and introduced the definition

$$\tilde{T}_{\mu\nu}^m \equiv -2 \frac{\delta \tilde{\mathcal{L}}_m}{\delta g^{\mu\nu}} + \tilde{\mathcal{L}}_m g_{\mu\nu}. \quad (8)$$

Now, the field equations become

$$\frac{M_p^2}{2} G_{\mu\nu} = T_{\mu\nu}^A + T_{\mu\nu}^m. \quad (9)$$

Note that we have passed over the arguments in all the functions for brevity. It is worth pointing out that the new matter energy-momentum tensor $T_{\mu\nu}^m$ can have, apparently, an additional non-vanishing pressure component if the vector fields have spatial components by virtue of the second term in eqn. (7). On the contrary, if we consider a time-like vector, there will be an additional contribution to the energy density as usually happens in kinetically coupled scalar models (see e.g [53]). Hence, $T_{\mu\nu}^m$ seems to be ambiguously defined in the sense that it depends on the components of the different A_μ^a . We shall discuss later this point and its implications to have a right interpretation of the cold dark matter component.

The coupled A_μ field equations of motion are obtained after varying the action with respect to A_μ^a . These can be written in the reduced form

$$\partial_\mu (\sqrt{-g} F^{a\mu\nu}) = 2\sqrt{-g} A^{\nu a} \left(V_{,\tilde{X}} + \frac{1}{2} \frac{f_{,X}}{f} \mathcal{L}_m \right). \quad (10)$$

As the conservation law sets the interacting term sourcing the continuity equation for each component without ambiguity, we find from here the general interacting expression for the coupling function (eqn. (3)) by taking the covariant derivative of eqn. (7):

$$\begin{aligned} \nabla_\mu T_\nu^{\mu m} &= -A_\beta^c \nabla_\mu A_c^\beta \left[\frac{f_{,X}}{f} (T_\nu^{\mu m} - f_{,X} A^{\mu a} A_{\nu a} \mathcal{L}_m) \right. \\ &\quad + \frac{f_{,XX}}{f} \mathcal{L}_m A_a^\mu A_\nu^a \left. \right] + \frac{f_{,X}}{f} A_c^\mu A_\nu^c [\nabla_\mu \mathcal{L}_m \\ &\quad + \frac{f_{,X}}{f} \mathcal{L}_m A_\beta^a \nabla_\mu A_a^\beta] + \frac{f_{,X}}{f} \mathcal{L}_m [A_\nu^c \nabla_\mu A_c^\mu \\ &\quad + A_c^\mu \nabla_\mu A_\nu^c], \end{aligned} \quad (11)$$

such that $\nabla_\mu T_\nu^{\mu m} = -\nabla_\mu T_\nu^{\mu A}$. Note that we have guaranteed the conservation of the uncoupled matter fluid $\nabla_\mu \tilde{T}_\nu^{\mu m} = 0$. It is worth noting that the general form of the interaction term depends explicitly on the vector fields and their first-order derivatives. In addition, it is valid for Abelian and non-Abelian vector fields since the coupling function only depends on A_μ^a and not, for instance, on the field strength tensor which involves the specific structure of the associated group. This alternative however suggests us to construct more general coupling functions, for instance, a coupling of the form $f(Y)$ where

$$Y \equiv -\frac{1}{4} F_{\mu\nu}^a F_a^{\mu\nu}, \quad (12)$$

so that the structure of the associated group becomes explicit⁴. This possibility clearly deserves further examination as well as the possibility to settle this idea in the context of vector-tensor theories through conformal/disformal transformations as manifestation of possible non-minimal couplings to gravity. Interesting frameworks to have in mind were recently developed for metric transformations based on a U(1) gauge field [56], on the field strength tensor [57] and on its dual tensor [58].

A. Particular setup: The cosmic triad

We consider a triad of mutually orthogonal and of the same norm space-like vector fields A_μ^a which is an arrangement compatible with isotropic and homogeneous background:

$$A_\mu^a \equiv a(t) A(t) \delta_\mu^a. \quad (13)$$

Here $A(t)$ is the common norm of the three vector fields and $a(t)$ is the scale factor in the FLRW spacetime with

⁴ For the particular case of SU(N) gauge fields, the self-interaction term that contributes to the kinetic energy, it being proportional to the coupling constant of the group, will appear now explicitly in both the gravitational field equations and the A_μ field equations.

line element $ds^2 = -dt^2 + a^2(t)\delta_{ij}dx^i dx^j$. Bearing this in mind, it is possible to compute the gravitational field equations and the A_μ field equations where the presence of the coupling function f is revealed:⁵

$$3M_p^2 H^2 = f\tilde{\rho}_m + \frac{3}{2}(\dot{A} + HA)^2 + V, \quad (14)$$

$$M_p^2(3H^2 + 2\dot{H}) = -\frac{1}{2}(\dot{A} + HA)^2 + V - 2V_{,\bar{X}}A^2 + f_{,X}A^2\tilde{\rho}_m, \quad (15)$$

$$\ddot{A} + \left(\frac{\ddot{a}}{a} + H^2\right)A + 3H\dot{A} + 2V_{,\bar{X}}A - f_{,X}A\tilde{\rho}_m = 0. \quad (16)$$

Here an upper dot denotes a derivative with respect to the cosmic time, $H(t) \equiv \dot{a}/a$ is the Hubble parameter, and $\tilde{\rho}_m$ is the cold dark matter energy density. As we assume a (pressureless) cold dark matter fluid, the last term in eqn. (15) can be interpreted as an effective pressure for the vector field arising from the coupling to matter. Consequently, we define the density and pressure of the vector field respectively as

$$\rho_A = \frac{3}{2}(\dot{A} + HA)^2 + V, \quad (17)$$

$$p_A = \frac{1}{2}(\dot{A} + HA)^2 - V + 2V_{,\bar{X}}A^2 - \frac{f_{,X}}{f}A^2\rho_m, \quad (18)$$

where we have introduced the definition $\rho_m \equiv f\tilde{\rho}_m$. It will be instructive to keep in mind that the energy density of the vector field is the result of the contribution of the kinetic term Y and the vector field potential V as in the canonical case; however, pressure has an additional contribution due to the coupling function. Such a contribution will be important whenever ρ_m does not vanish, affecting consequently the total energy budget of the universe (see eqn. 14). Indeed, as we shall see, the kinetic term will contribute early as dark radiation $p_A = p_Y = \frac{1}{3}\rho_Y$ as expected commonly for space-like vector fields, while the potential will work as DE to account for the late-time accelerated expansion.

From eqns. (17)-(18), it is possible to write the A_μ field equation (eqn. 16) in the form of the continuity equation for a fluid, allowing us to infer the interacting term:

$$\dot{\rho}_A + 3H(\rho_A + p_A) = 3A\dot{A}\frac{f_{,X}}{f}\rho_m, \quad (19)$$

$$\dot{\rho}_m + 3H\rho_m = -3A\dot{A}\frac{f_{,X}}{f}\rho_m. \quad (20)$$

The continuity equations evidence clearly that both components interact with each other through a novel interaction term $Q = -\frac{3f_{,X}}{f}\rho_m$ which is very similar to the interaction term derived from the coupled tachyonic dark energy model [59].

As we are mostly interested in the late-time cosmology, we define the effective state parameter from eqn. (15) as follows

$$w_{\text{eff}} \equiv \frac{p_T}{\rho_T} = -\left(1 + \frac{2\dot{H}}{3H^2}\right), \quad (21)$$

where p_T and ρ_T are respectively the total pressure and energy density, and search accordingly for the condition $w_{\text{eff}} < -1/3$ in such a period. This parameter will describe the transition from the domination of each component in accordance to the evolution of the universe. It is also important to define the state parameter for the vector field as $w_A \equiv \frac{p_A}{\rho_A}$ which will coincide with w_{eff} at early and late times as we will see. We have thereby provided all the key equations needed to describe the cosmological background dynamics. We will first address this issue in a qualitative way by using the dynamical systems approach in the next section. Then, we will numerically solve the coupled system to visualize the cosmic evolution in section IV.

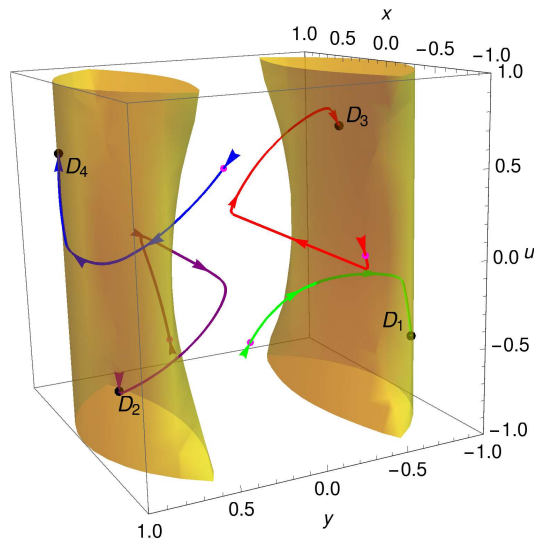


FIG. 1. Trajectories for different initial conditions (cyan points) in phase space converging to the attractor solutions $D_{1,2,3,4}$ (black points). These trajectories correspond to numerical solutions of the dynamical system in eqn. (25), after dimensional reduction, for the parameters $q = -0.1$ and $\lambda = 0.4$. The light yellow region denotes the physical region we define as the intersection of the physical phase space and the region where the universe undergoes a standard accelerated expansion ($w_{\text{eff}} < 1/3$), the latter's being more restrictive.

⁵ This realization results in an interesting generalization of the pioneering model of ref. [39] and opens up a wide possibility to build coupled dark energy models driven only by vector fields.

TABLE I. Fixed points of the autonomous system in eqn. (25) and their main physical features. The dynamical stability is found by demanding the standard requirement of negativity of the eigenvalues of the Jacobian matrix \mathcal{M} associated to the linear system evaluated at the critical points (see Appendix). In addition, the density parameter associated to the cosmic triad, the latter's state parameter, the effective state parameter, the conditions for the existence of the critical points in phase space, and the conditions for supporting late-time accelerated expansion are displayed as indicated.

Point	x_c	y_c	z_c	u_c	Ω_A	w_A	w_{eff}	Existence	Acceleration
A_{\pm}	± 1	0	0	$\pm\sqrt{2}$	1	1/3	1/3	$\forall q, \lambda$	No
B_{\pm}	$\pm \frac{\sqrt{2q}}{\sqrt{-1+2q}}$	0	$\pm \frac{1}{\sqrt{1-2q}}$	$\pm\sqrt{2}x_c$	$\frac{2q}{-1+2q}$	0	0	$\forall q, \lambda < 0$	No
$D_{1,2}$	$-\frac{\sqrt{-1+3\lambda}}{\sqrt{3\lambda}}$	$\mp \frac{1}{\sqrt{3\lambda}}$	0	$-\sqrt{2}x_c$	1	-1	-1	$\forall q, \lambda > 1/3$	$\forall q, \lambda$
$D_{3,4}$	$\frac{\sqrt{-1+3\lambda}}{\sqrt{3\lambda}}$	$\mp \frac{1}{\sqrt{3\lambda}}$	0	$\sqrt{2}x_c$	1	-1	-1	$\forall q, \lambda > 1/3$	$\forall q, \lambda$

III. DYNAMICAL SYSTEM

In order to study the background evolution of the model given by eqns. (14)-(16) and eqns. (19)-(20) by the dynamical system analysis, we transform the system of equations into an autonomous system of first-order differential equations. To do so, we introduce the following dimensionless variables that will define the phase space portrait:

$$\begin{aligned} x &\equiv \sqrt{\frac{(\dot{A} + HA)^2}{2M_p^2 H^2}}; & y &\equiv \sqrt{\frac{V}{3M_p^2 H^2}}; \\ z &\equiv \sqrt{\frac{\rho_m}{3M_p^2 H^2}}; & u &\equiv \frac{A}{M_p}. \end{aligned} \quad (22)$$

These variables satisfy, in turn, the Friedmann constraint

$$x^2 + y^2 + z^2 = 1. \quad (23)$$

At this point, it is necessary to define the functional forms of both the potential and the coupling function. For the former, we set an exponential potential while, for the latter, we set a power law⁶:

$$V(\tilde{X}) = V_0 e^{-\lambda \tilde{X}/M_p^2}, \quad f(X) = \left(\frac{X}{M_p^2}\right)^q, \quad (24)$$

such that $\frac{V_{,\tilde{X}}}{V}$ and $\frac{f_{,X}}{f}$ are completely determined as demanded to close the system of coupled equations. Here λ and q are the dimensionless model parameters to be constrained. With all this at disposition, we derive the

autonomous system

$$\begin{aligned} x' &= -x \left(2 + \frac{H'}{H} \right) \\ &\quad + \frac{1}{x} \left[3\lambda y^2 u^2 - \sqrt{2} \frac{x}{u} q z^2 - y \left(y' + y \frac{H'}{H} \right) \right], \\ y' &= -y \left[\frac{H'}{H} + 3u^2 \lambda \left(\sqrt{2} \frac{x}{u} - 1 \right) \right], \\ z' &= -z \left[\frac{H'}{H} + \frac{3}{2} - q \left(\sqrt{2} \frac{x}{u} - 1 \right) \right], \\ u' &= \sqrt{2}x - u. \end{aligned} \quad (25)$$

Here the prime denotes a derivative with respect to $N \equiv \ln a$. We also determine the accelerating equation eqn. (15) in terms of the dimensionless quantities:

$$\frac{H'}{H} = -\frac{3}{2}(1 + w_{\text{eff}}), \quad (26)$$

with

$$w_{\text{eff}} = \frac{x^2}{3} - y^2 - 2\lambda y^2 u^2 + \frac{2}{3} q z^2, \quad (27)$$

where the presence of the interacting term via the parameter q and the quantity z in the above equation is clear, evidencing thus the coupling of the vector field to matter. The state parameter for the vector DE is, in the same fashion,

$$w_A = \frac{x^2/3 - y^2 - 2\lambda y^2 u^2 + \frac{2}{3} q z^2}{x^2 + y^2}. \quad (28)$$

To ease our computations, we reduce the 4-dimensional phase space to a 3-dimensional one through the Friedmann constraint. The physical volume of the reduced phase space becomes then $x^2 + y^2 \leq 1$ (with u unconstrained). In what follows, we will compute the critical points of the system and study the general conditions that determine both their dynamical character and their existence in phase space, following the standard procedure of the dynamical systems theory.

⁶ The reason for this choice is mainly technical as it makes easier to write the autonomous system, rendering the physical space compact in turn. This fact guarantees that trajectories do not extend to infinity.

A. Phase space trajectories

In order to better comprehend the dynamical character of the appearing solutions, we have first drawn some parametric trajectories in phase space for different initial conditions (marked as cyan points) in fig. 1. These points are initially close to a radiation dominated universe. As time passes the trajectories bring near some points (presumably saddle in nature) before being finally attracted towards four possible attractor solutions given by the critical points⁷ $(x_{c,i}, y_{c,i}, u_{c,i})$. The latter, as seen in fig. 1, are located in accordance to the odd-parity invariance of the system (see Table I) and coloured black inside the physical region. Such a physical region is denoted by light yellow and it is defined as the intersection space of the physical reduced phase space $x^2 + y^2 \leq 1$ and the region where the universe undergoes a standard accelerated expansion ($w_{eff} < 1/3$), with u now constrained by eqn. (27). One couple of solutions are, as a first criterion, located according to the sign of the parameter u . For instance $D_{1,2}$ correspond to u negative while, for the opposite sign, we have the attractors $D_{3,4}$. Nevertheless, they all have the same physical meaning: de Sitter-type attractors characterized by the dominance of vector DE through its potential. We have chosen $q = -0.1$ and $\lambda = 0.4$ for these numerical solutions. However, we have checked that the location of the attractor solutions inside the physical region does not depend on q but does on λ . Indeed, by increasing λ significantly, the attractor points are slightly shifted from $y = \pm 1$ towards $y = 0$, these being now enclosed by the renewed cylinder-shaped regions. Regarding the effect of q , it turns out to be important only in an intermediate stage of the universe when matter starts dominating. This leads to a non-vanishing vector energy density contribution that can alter the dynamic expansion other than having some impact on non-linear processes of the early universe as the formation of cosmic structures. All of the above dynamical features will be more evident in the two-dimensional stream plots that we will display next as well as in the performed numerical computation that will be described in section V.

B. Critical points and stability

The critical points are computed by matching to zero each equation of the autonomous system and solving a set of simple algebraic expressions. The solutions are shown in Table I corresponding to eight critical points. However, as we have discussed previously, they can be

⁷ Indeed, these solutions are doubly degenerate in the sense that they all represent one single physical solution of cosmological interest due to the symmetry of the invariant phase space. The emergence of these solutions, and their differences, are due to different sign combinations for the fixed points $(x_{c,i}, y_{c,i}, u_{c,i})$ with i running from 1 up to 4, as can be seen in Table. I.

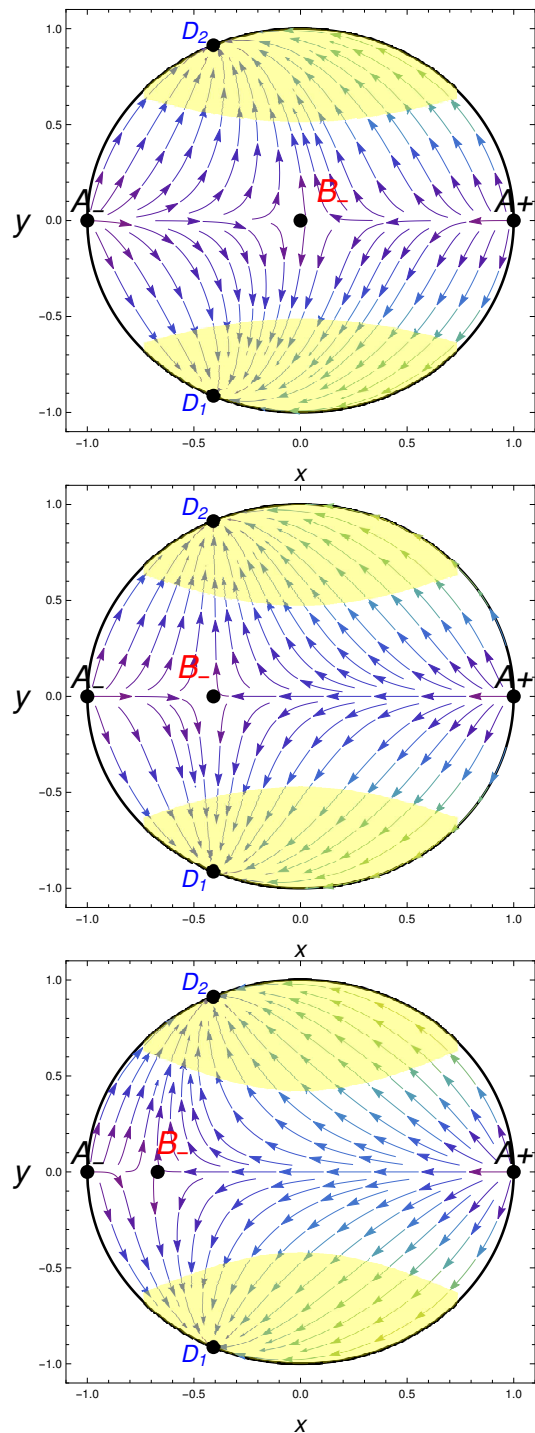


FIG. 2. Reduced phase space of the dynamical system. We have set the slice $u_c = -|u_c| = -\frac{\sqrt{-2/3+2\lambda}}{\sqrt{\lambda}}$, corresponding to $D_{1,2}$ and have taken $\lambda = 0.4$ and $q = 0, -0.1, -0.2$ in the top, middle and bottom panels respectively. The light yellow region denotes as before the physical region where the condition $x^2 + y^2 \leq 1$ is satisfied along with the condition for the accelerated expansion.

reduced without ambiguities to three physical solutions of cosmological interest, each one playing a crucial role

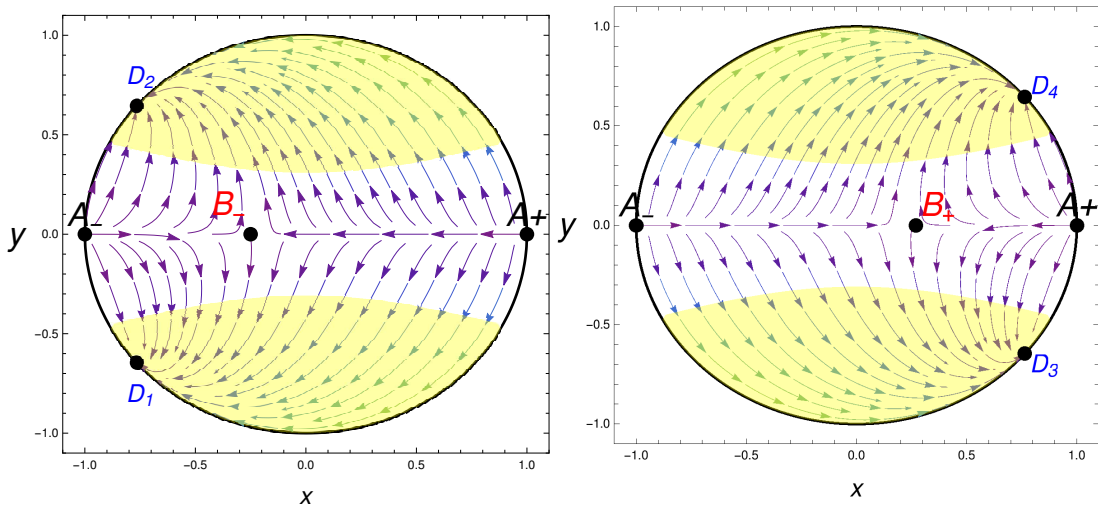


FIG. 3. Reduced phase space of the dynamical system. We have set the slice $u_c = -|u_c|$ for the left panel and $u_c = |u_c|$ for the right panel in order to appreciate the equivalence between these two solutions which correspond to the attractors $D_{1,2}$ and $D_{3,4}$, respectively. It is also important to note how the attractor points approach A_{\pm} when we choose a larger value for λ ($\lambda = 0.8$) while keeping q fixed ($q = -0.1$). The light yellow region denotes the physical region where the universe is accelerating.

in the evolution of the universe. We will refer then to a single solution when they exhibit the same physical features. Some physical quantities are also displayed in the table for a better description of the dynamical behavior of the system such as the vector density parameter, the vector state parameter, the effective state parameter, the conditions for the existence of the critical points, and whether they correspond to an accelerated expansion period. The existence is determined by the requirement that $0 \leq x^2 + y^2 \leq 1$ and that the coordinates of the critical points must be real valued. Interestingly, there exists a new scaling solution mediated by the parameter q (fixed point B_{\pm}). The emergence of this solution is due to the presence of the kinetic energy x_c of the vector field during the matter dominated epoch contrary to the uncoupled case $q = 0$ ($x_c = 0$). This remarkable difference may lead to interesting implications not only at the background level, aiming at addressing the coincidence problem and the Hubble tension, but also at the linear/non-linear regime in perturbations, affecting for instance the formation and evolution of cosmic structures in the universe. This point will be discussed later in view of the cosmological observations. We discuss the main physical features of each fixed point as follows:

- **Point (A_{\pm}):** this *saddle point* corresponds to a kinetic dominated solution or dark radiation since x is the only non-zero dynamical variable of the system. Hence, the cosmic triad fully dominates the energy density budget in the form of dark radiation with $w_A = 1/3$ and $\Omega_A = 1$. We conclude that this point represents a *radiation dominated period* with effective state parameter $w_{\text{eff}} = 1/3$ and that acceleration is not realizable during this initial stage. As can be seen in Table I and the Appendix, there is no explicit dependence of the existence and the

stability conditions of this critical point on the parameter values.

- **Point (B_{\pm}):** Though this point exists in the uncoupled case ($q = 0$), the total energy density of the universe is not totally governed by matter ($\Omega_m = \frac{1}{1-2q}$) in this intermediate stage when $q \neq 0$. Instead, we have an outstanding contribution of the vector field ($\Omega_A = \frac{2q}{-1+2q}$ with $q \neq 1/2$) due to its coupling to matter through the parameter q . We may refer to this fixed point as the *coupled multi-Proca vector-matter fixed point*. Despite the contribution of the vector field to the total energy budget, this *saddle point* represents matter domination with $w_{\text{eff}} = 0$ and with the vector field acting as a dust-like fluid. This shows that acceleration is not realizable unless the potential (y_c) dominated solution is achieved. On the other hand, one of the conditions for the existence of this point is simply $\lambda < 0$. In addition, this preliminary inspection tells us that, in order to have well defined (real valued) positive energy density values for both components, the parameter q must be negative. Nonetheless, feasible numerical solutions include also positive q values as we will see. The most noticeable physical aspect of this solution is that it represents a novel scaling solution where the dark energy density to matter energy density ratio scales as $\rho_{DE}/\rho_m \propto -2q$, and has interesting implications at the background level aiming to solve the coincidence problem. This solution may be seen as a generalization of the pioneering dark energy model based on the cosmic triad [39].
- **Point (D_i):** This critical point is a *dynamical stable attractor* with all negative eigenvalues. Interest-

ingly, this point exhibits an accelerated period with state parameter $w_A = w_{eff} = -1$ independent entirely of the model parameters. Despite the explicit dependence of w_{eff} on q and λ in eqn. (27), there appears an intriguing cancellation when replacing this critical point. This renders, as an attractor solution, a de Sitter universe with $w_{eff} = -1$ at late times as shall be verified numerically. In other words, the vector field mimics DE at late times with density parameter $\Omega_A = x_{c,i}^2 + y_{c,i}^2 = 1$ being also independent of the model parameters.

In summary, the model we propose in this work provides a cosmological evolution where the cosmic triad contributes in the form of dark radiation at early times, with a significant presence of its kinetic energy (scaling solution) quantified by the coupling q at the matter domination era, and mimicking DE at late times (low redshift) through the exponential potential.

To see the dynamical evolution of the system characterized by such fixed points, we display the reduced phase space portrait of the dynamical system eqn. (25) in fig. 2 for the same parameter values as in fig. 1 (except for q that takes several values as indicated in the caption). These two-dimensional plots are obtained by setting the slice $u = u_c$ at the attractor point D_i . Notice that a negative u_c determines the physical region enclosing D_1 and D_2 ; on the contrary, we have the equivalent physical region enclosing the points D_3 and D_4 as can be ascertained in fig. 3 (see also fig. 1). Namely, the corresponding phase spaces have the same physical meaning as we already discussed. For the sake of easiness, we restrict our attention to the case with negative u in all the subsequent plots, which corresponds to portraying $D_{1,2}$ and the saddle points A_{\pm} and B_{\pm} . Thus, all trajectories leaving the saddle point A_+ (dark radiation), with some of them passing close to B_- (scaling solution) move towards one of the attractor solutions, D_1 or D_2 , (downwards or upwards, respectively), which accounts for an accelerated expansion period as can be seen in fig. 2. In the same plot, the light yellow contour indicates the region where acceleration is realizable which remarkably occurs for any set of values for the model parameters. In addition, we can see that the effect of varying q is noticed only by a slight shift in B_- and not on $D_{1,2}$. It is evident that, for $q = 0$, $B_- = B_+$ at $x_c = 0$; this uncoupled case corresponds to the top panel of fig. 2.

We end this part by analyzing the effect of changing λ . As expected from Table I, the attractor points $D_{1,2}$ ($D_{3,4}$) move along the black boundary towards A_- (A_+) when we increase λ . This behaviour can be appreciated in fig. 3 where we have taken $\lambda = 0.8$ in contrast to the case $\lambda = 0.4$ depicted in fig. 2. As a further remark about this analysis, we note that each component of the total energy density is given by a well-characterized state parameter at each fixed point which means that there is no any dependence on the model parameters even though they control the whole dynamical behaviour of w_{eff} . The parameter λ affects, for instance, the value for w_{eff} at

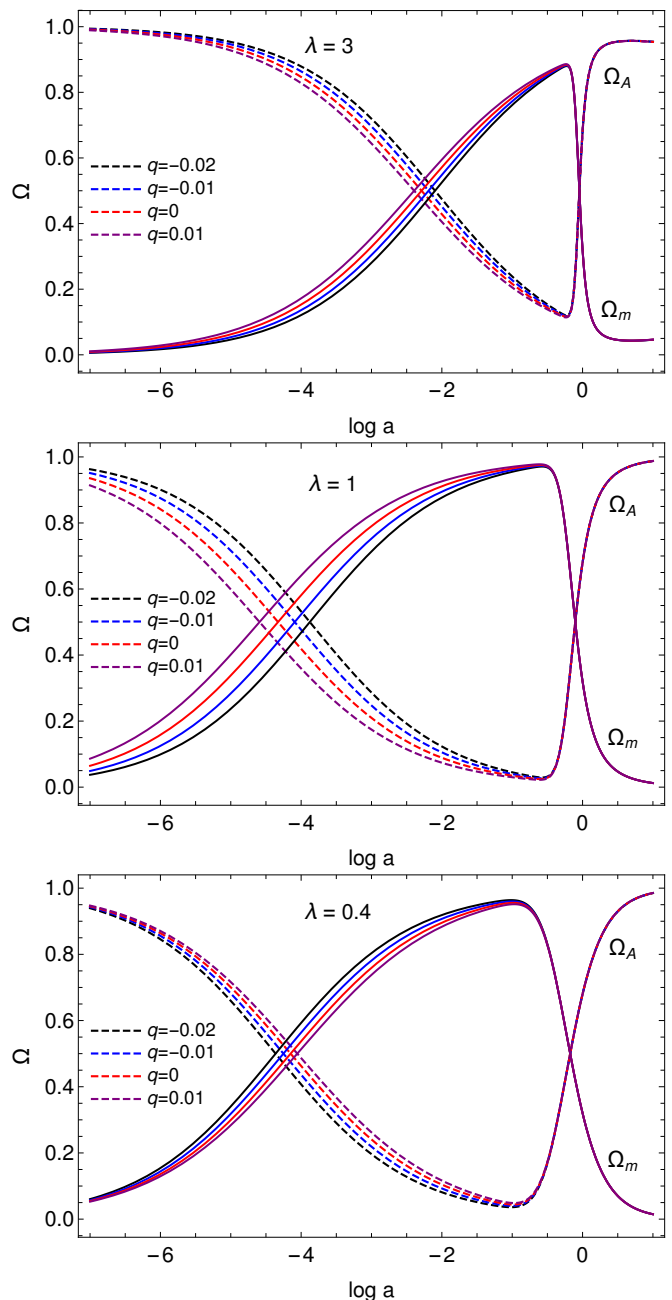


FIG. 4. Evolution of Ω_A and Ω_m versus the number of e-folds $N \equiv \log a$ for different values of q . Dashed and solid lines denote solutions for Ω_A and Ω_m respectively. Top, middle and bottom panels correspond to $\lambda = 3, 1$, and 0.4 respectively. We have chosen $u^{(0)} = 0.9$ as a comparable value with respect to the $x^{(0)}$ and $y^{(0)}$ values. The other initial conditions have been chosen to match the present value $\Omega_A = \Omega_{DE}^{(0)} = 0.68$.

the onset of matter domination. These features will be appreciated in the next section when we numerically solve the cosmological evolution of the system in terms of the parameters of the model.

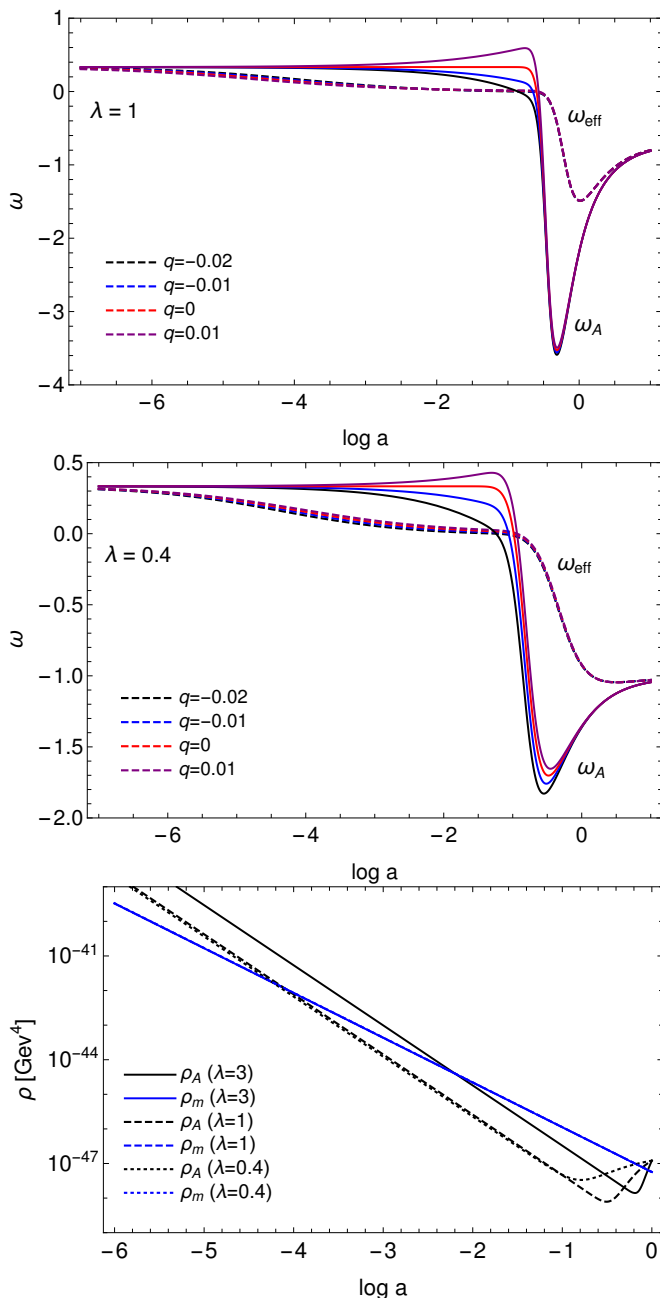


FIG. 5. Evolution of the state parameters versus the number of e-folds N in the top and middle panels with $\lambda = 1$ and 0.4 , respectively, for different values of q as can be read in the legends. Dashed and solid lines denote solutions for w_{eff} and w_A respectively. We show the evolution of the energy density for each component in the bottom panel for $q = -0.1$ and different values of λ as indicated in the legends. We have chosen $u^{(0)} = 0.9$ as a comparable value with respect to the $x^{(0)}$ and $y^{(0)}$ values. The other initial conditions have been chosen to match the present value $\Omega_A = \Omega_{DE}^{(0)} = 0.68$.

IV. NUMERICAL RESULTS: COSMOLOGICAL BACKGROUND EVOLUTION

We employ numerical methods in this section to solve the cosmological evolution of the model in order to verify the dynamical behaviour found in the previous section. We start by exploring the viable region of the parameter space in accordance with the analysis already performed. After an exhaustive exploration of the numerical solutions in terms of the model parameters, we notice that the behaviour of the density parameters associated to the vector field Ω_A and the matter component Ω_m is mostly influenced at very high redshift (i.e., large and negative e-folding N) by the parameter λ in the range $1/3 < \lambda < 1$, displaying an early matter-dark radiation equality (see middle and bottom panels of fig. 4). Meanwhile, for $\lambda > 1$, they display important changes with respect to the former at very low redshift as can be observed in fig. 4 top panel. Importantly, the most notorious difference among the numerical solutions shows at the full matter domination epoch: for $\lambda > 1$ the matter density parameter is always below one because of the non-vanishing vector energy contribution leading, for instance, to $\Omega_m \sim 0.9$ for the case $\lambda = 3$ (see top panel of fig. 4). In contrast, for $\lambda < 1$, $\Omega_m \approx 1$. In general, by increasing λ an order of magnitude, the matter density is reduced roughly 10%. It is also worth pointing out that, for $\lambda > 3$, the transition between matter and DE domination occurs at $z < 0.1$, i.e. very close to the present epoch, resulting in a cosmic coincidence situation. In short, as λ increases, the matter-dark energy equality is slightly shifted to the present epoch. Hence, there should be an upper limit for λ to have a successful dynamic expansion such that the coincidence appears much less severe today. As a conservative limit we set λ to be $\mathcal{O}(1)$ but a more stringent limit will be derived by the use of observational data.

The effect of changing q is notoriously amplified in the numerical solutions with $\lambda = 1$ (compare the middle panel with the other two in fig. 4) and, in particular, around matter-dark radiation equality but with almost indistinguishable differences at the very early epoch and shortly before today even for any value of λ . A consequence of this is the convergence of the energy-density solutions for all q values (including the uncoupled case $q = 0$) at the aforementioned epochs as can be appreciated in the same figure. In other words, the effect of q turns out to be noticeable in an intermediate stage of the universe evolution; in contrast, it is turned off in other stages as we have already assessed in the dynamical system analysis presented in section III. Interestingly, all the numerical solutions exhibit, as a general trend, an early contribution of the vector field in the form of dark radiation and a late contribution in the form of DE. To put it in another way, the kinetic energy and the potential of the vector fields dominate at early and late times respectively, with the possibility, provided that $q \neq 0$, of having an early contribution of the cosmic triad to the total en-

ergy density during the matter domination. This could leave some imprints on the structure formation that can be confronted with observations.

It is very instructive to display how the effective state parameter and the one for the vector field evolve with time. This allows us to more clearly observe the dominance of each component, with particular attention on the tracking solutions $w_r \rightarrow w_m \rightarrow w_{DE}$ ensuring sequentially (dark) radiation, matter, and DE transitions. In fact, it is appealing to see how w_A tracks w_{eff} at very high and low redshifts. This result is shown in fig. 5 for two particular values of λ . Both cases exhibit a well behaved transition of w_{eff} from dark radiation to matter and then to DE domination. In particular, the case $\lambda = 1$ in the top panel shows an absolute minimum for w_{eff} before it reaches a value $w_{eff} = -1$. The same panel shows, in addition, a deeper downfall of w_A contrary to the case $\lambda = 0.4$ in the middle panel. Indeed, the most significant effect of λ on the dynamical evolution of the universe is towards the onset of the accelerated expansion epoch until the minimum of w_A due to the dominance of the potential energy in such a period, as expected from the equations of state (27) and (28). In physical terms, the vector field displays a phantom behaviour before achieving the de Sitter regime. Later, after the oscillation, the vector field essentially freezes with $\rho_A = V = \text{const.}$ and the Hubble parameter becomes constant as can be inferred from the density parameters shown in fig. 4.

To sum up things, the cosmic triad exposes two outstanding features during the evolution of the universe. At early times, during radiation era, it tracks $w_{eff} \rightarrow w_A = -1/3$, contributing thus to radiation in the form of dark radiation whereas, at late times, it changes its role to DE, providing a de Sitter-type accelerated solution with $w_{eff} \rightarrow w_A = -1$. Let us now point out that the effect of q on the numerical solutions is rather significant for w_A at the matter domination era in accordance with the dependence of the state parameter in eqn. (28) via the qz^2 term which accounts for the matter energy density.

Finally, we plot the energy density for both components and investigate the effects of the model parameters during the evolution of the universe in the bottom panel of fig. 5. From here, we conclude that the only significant change occurs for ρ_A (black curves); in particular the solution with $\lambda = 3$ (solid black curve) is quite distinguishable from the solutions $\lambda = 0.4$ and $\lambda = 1$ along the whole evolution. These latter solutions are however distinct each other only at very low-redshift as can be appreciated. Hence, comparing the distinct numerical solutions, we notice that those distinguishable features are due to the influence of the potential at low redshift, resulting in a deeper downfall for the cases $\lambda = 1$ and $\lambda = 3$ consistent with the dynamics of w_A (see, for instance, how deep is the solution with $\lambda = 1$ in contrast to the one with $\lambda = 0.4$). Interestingly, both ρ_A and ρ_m match twice: the first match (dark radiation-matter equality) occurs around $z \approx 60$ ($N = -\log(1+z)$) for dotted ($\lambda = 0.4$) and dashed ($\lambda = 1$) black curves and

$z \approx 7$ for the solid ($\lambda = 3$) black curve, whereas the second match (matter-dark energy equality) happens close to the present epoch as we have discussed when analyzing the energy densities in fig. 5. We argue then that these solutions are not finely tuned in view of the coincidence problem due to the dominance of the potential during the accelerated period.

V. DISCUSSION AND CONCLUSIONS

We proposed a novel coupling between multi-Proca vector fields and cold dark matter at the level of the action through a vector mass-type term. The general interacting term in a FLRW universe, with the cosmic triad configuration for the space-like vector fields, is of the form $Q = -\frac{3f_x}{f}\rho_m$, it being fully independent of the vector field nature (i.e., the specific structure of the associated group is not manifest, see eqn. (11)).

The dynamical system analysis revealed the existence of three physical critical points corresponding to a dark radiation behaviour with $\Omega_A = 1$ (saddle point), a coupled multi-Proca vector-matter behaviour or simply a scaling solution where the density ratio scales as $\rho_{DE}/\rho_m \propto -2q$ (saddle point), and a DE behaviour leading to an accelerated expansion period with $\Omega_A = \Omega_{DE}$ (de Sitter-type attractor). These transitions can easily be seen in the phase space orbits in fig. 2 and fig. 3.

For completeness, we also performed numerical computations of the density parameters and the effective state parameter to verify the evolution of the universe and to more clearly investigate the effects of the model parameters q and λ . As an interesting result, we found an appealing behaviour for the energy density associated to the vector fields that can naturally alleviate the coincidence problem due to the emergence of the potential at low redshift with no fine tuning. Indeed, for $\lambda = 3$, ρ_A is at most two orders of magnitude larger than ρ_m in the past (high redshift), those differences being even smaller across the whole cosmic history for $\lambda = 1$ as can be seen in the bottom panel of fig. 5.

As future theoretical research, we propose building more general couplings involving, for instance, the field strength or its dual in order to make the structure of the group explicit. Moreover, though our proposal is not formally framed in the context of conformal transformations, it would be worth investigating the respective vector transformation in the context of vector tensor theories as was recently done for U(1) vector fields [56] and the extended vector-tensor theories [60].

To conclude, we proposed in this work a novel coupling to matter that allows the multi-Proca vector fields to exist during the matter dominated epoch, exhibiting consequently a novel scaling solution which is cosmologically appealing in order to address the coincidence problem and the debated Hubble tension. Though we did not attack directly such an issue in this work, it would be worth examining it in a future work whether this model

may conciliate the observational data at high and low redshift. This would serve as a first challenge to put the model in a phenomenological context and to constrain also the background quantities. Likewise, the effects of such a coupling could be important in the evolution of matter density perturbations and all the derived quantities associated with measurements of large-scale structures such as the growth rate and the redshift-space distortion $f\sigma_8$. Hence, the subsequent observational test would be to constrain the evolution of matter perturbations and the evolution of gravitational potentials by including redshift-space distortion measurements from different observational surveys. Another important examination within the context of structure formation would be to investigate the influence of such a coupling on the spherical collapse and number counts at the corresponding redshift. Regarding the dark radiation effects in the early-universe physics (see e.g. [61–65]), they can imprint detectable signatures in the cosmic microwave background radiation causing both spectral distortions and additional anisotropies. In addition, they can contribute to the effective number of relativistic species N_{eff} as was studied in a dark energy model whose action is composed of non-Abelian gauge fields [66]. Our plan is to address these concerns in a forthcoming publication in order to guarantee the consistence of the model throughout the different stages of the universe.

ACKNOWLEDGMENTS

L. G. G is supported by the Postdoctoral Fellowship Program N° 2020000102 of the Vicerrectoría de Investigación y Extensión - Universidad Industrial de Santander. This work was supported by the following grants: Colciencias-Deutscher Akademischer Austauschdienst Grant No. 110278258747 RC-774-2017 and Dirección de Investigación y Extensión de la Facultad de Ciencias - Universidad Industrial de Santander Grant No. 2460. L. G. G acknowledges Departamento de Física - Universidad del Valle for its hospitality at early stages of this project and in particular César A. Valenzuela-Toledo for stimulating discussions during his scientific visit. L. G. G dedicates this work to the memory of his dear friend and colleague Diego Leonardo Cáceres Uribe who passed away so unexpectedly: your essence shall endure forever among us.

Appendix: Stability conditions

We show in this appendix the general conditions that render the phase space portrait stable. The stability analysis follows the standard criteria of finding the eigenvalues of the Jacobian matrix \mathcal{M} associated to the linear system and classifying them according to the stability

criteria. This allows us to establish the dynamical character of the fixed points and, therefore, their cosmological viability.

The matrix elements of \mathcal{M} are:

$$\begin{aligned}\mathcal{M}_{11} &= \frac{2qx(\sqrt{2}-ux)}{u} - q(-1+x^2+y^2) \\ &\quad + \frac{-1+3x^2-y^2(3+6u^2\lambda)}{2}, \\ \mathcal{M}_{12} &= \frac{2q(\sqrt{2}-ux)y}{u} + \frac{12\sqrt{2}uy\lambda - 2xy(3+6u^2\lambda)}{2}, \\ \mathcal{M}_{13} &= -\frac{qx(-1+x^2+y^2)}{u} - \frac{q(\sqrt{2}-ux)(-1+x^2+y^2)}{u^2} \\ &\quad + \frac{6\sqrt{2}y^2\lambda - 12uxy^2\lambda}{2}, \\ \mathcal{M}_{21} &= -\frac{y(-2x+4qx+6\sqrt{2}u\lambda)}{2}, \\ \mathcal{M}_{22} &= -\frac{y(4qy+6y(1+2u^2\lambda))}{2} \\ &\quad + \frac{x^2-2q(-1+x^2+y^2)-6\sqrt{2}ux\lambda-3(-1+y^2)(1+2u^2\lambda)}{2}, \\ \mathcal{M}_{23} &= -\frac{y(6\sqrt{2}x\lambda+12u(-1+y^2)\lambda)}{2}, \\ \mathcal{M}_{31} &= \sqrt{2}, \\ \mathcal{M}_{32} &= 0, \\ \mathcal{M}_{33} &= -1.\end{aligned}$$

Thus, the fixed points and their characterization are as follow:

- Fixed points (A_{\pm}):
 $e_1 = 2, e_2 = -1, e_3 = 1$.
 These points clearly represent saddle points since the eigenvalues are real valued with two of them having opposite signs.
- Fixed points (B_{\pm}):
 $e_1 = \frac{3}{2}, e_{2,3} = \frac{3-6q\pm\sqrt{7}\sqrt{-1+4q-4q^2}}{4(-1+2q)}$.
 It is straightforward to verify that $e_{2,3}$ are always negative for any value of q such that these fixed point are also saddle points.
- Fixed points (D_i): The corresponding eigenvalues e_i are quite long and little illuminating to be reported here as a guidance for analytical treatment. Their real parts are plotted instead in terms of the parameter λ in fig. 6 where the conditions $\lambda < 0$ and $\lambda > 1/3$ are read off as a requirement for having $\text{Re}[e_i] < 0$. Hence, these fixed points are stable representing dynamical attractors. The condition $\lambda > 1/3$ guarantees, in turn, their cosmological viability as can be seen in Table. I.

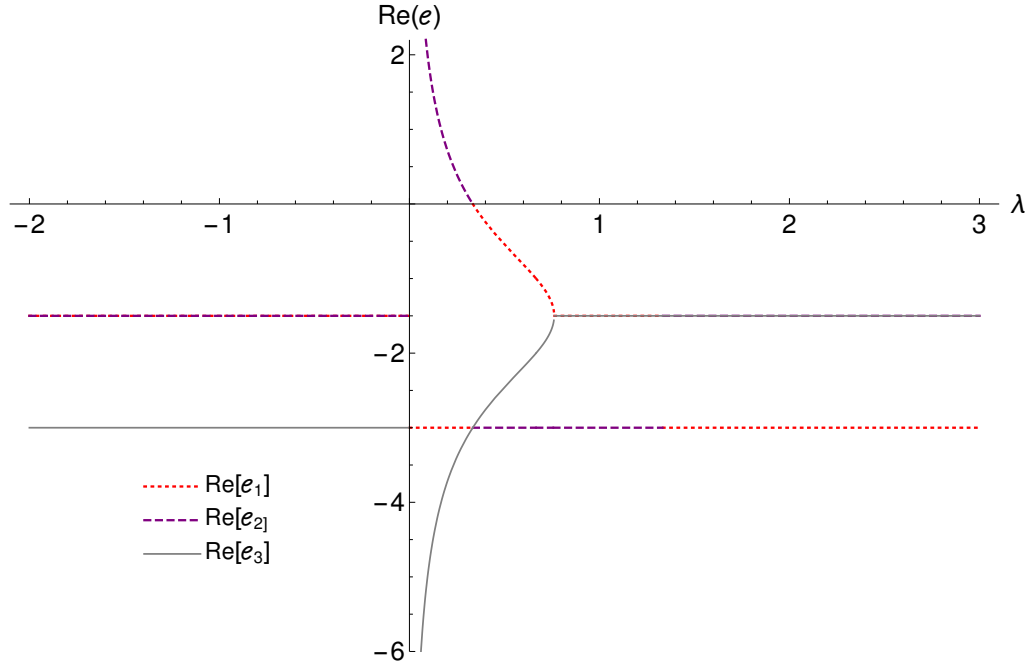


FIG. 6. Real part of the eigenvalues of the matrix \mathcal{M} associated to the fixed points D_i in one-dimensional phase space. Negative values for $\text{Re}[e_i]$ guarantee the stability of the critical points.

-
- [1] N. Aghanim *et al.* (Planck), (2018), arXiv:1807.06209 [astro-ph.CO].
- [2] A. G. Riess *et al.* (Supernova Search Team), *Astron. J.* **116**, 1009 (1998), arXiv:astro-ph/9805201.
- [3] B. P. Schmidt *et al.* (Supernova Search Team), *Astrophys. J.* **507**, 46 (1998), arXiv:astro-ph/9805200.
- [4] S. Perlmutter *et al.* (Supernova Cosmology Project), *Astrophys. J.* **517**, 565 (1999), arXiv:astro-ph/9812133.
- [5] S. Weinberg, *Rev. Mod. Phys.* **61**, 1 (1989).
- [6] L. Amendola and S. Tsujikawa, *Dark Energy* (Cambridge University Press, 2015).
- [7] E. Di Valentino, A. Melchiorri, and J. Silk, *Nat. Astron.* **4**, 196 (2019), arXiv:1911.02087 [astro-ph.CO].
- [8] E. Macaulay, I. K. Wehus, and H. K. Eriksen, *Phys. Rev. Lett.* **111**, 161301 (2013), arXiv:1303.6583 [astro-ph.CO].
- [9] R. A. Battye, T. Charnock, and A. Moss, *Phys. Rev.* **D91**, 103508 (2015), arXiv:1409.2769 [astro-ph.CO].
- [10] S. Alam *et al.* (BOSS), *Mon. Not. Roy. Astron. Soc.* **470**, 2617 (2017), arXiv:1607.03155 [astro-ph.CO].
- [11] T. M. C. Abbott *et al.* (DES), *Phys. Rev.* **D98**, 043526 (2018), arXiv:1708.01530 [astro-ph.CO].
- [12] W. L. Freedman, *Nat. Astron.* **1**, 121 (2017), arXiv:1706.02739 [astro-ph.CO].
- [13] A. G. Riess *et al.*, *Astrophys. J.* **876**, 85 (2019), arXiv:1903.07603 [astro-ph.CO].
- [14] T. Clifton, P. G. Ferreira, A. Padilla, and C. Skordis, *Phys. Rept.* **513**, 1 (2012), arXiv:1106.2476 [astro-ph.CO].
- [15] J. M. Ezquiaga and M. Zumalacregui, *Front. Astron. Space Sci.* **5**, 44 (2018), arXiv:1807.09241 [astro-ph.CO].
- [16] D. Lovelock, *J. Math. Phys.* **12**, 498 (1971).
- [17] P. Horava, *Phys. Rev.* **D79**, 084008 (2009), arXiv:0901.3775 [hep-th].
- [18] C. Wetterich, *Nucl. Phys.* **B302**, 668 (1988), arXiv:1711.03844 [hep-th].
- [19] B. Ratra and P. J. E. Peebles, *Phys. Rev.* **D37**, 3406 (1988).
- [20] C. Armendariz-Picon, T. Damour, and V. F. Mukhanov, *Phys. Lett.* **B458**, 209 (1999), arXiv:hep-th/9904075.
- [21] C. Armendariz-Picon, V. F. Mukhanov, and P. J. Steinhardt, *Phys. Rev. Lett.* **85**, 4438 (2000), arXiv:astro-ph/0004134.
- [22] C. Armendariz-Picon, V. F. Mukhanov, and P. J. Steinhardt, *Phys. Rev.* **D63**, 103510 (2001), arXiv:astro-ph/0006373.
- [23] G. W. Horndeski, *Int. J. Theor. Phys.* **10**, 363 (1974).
- [24] G. W. Horndeski, *J. Math. Phys.* **17**, 1980 (1976).
- [25] A. Nicolis, R. Rattazzi, and E. Trincherini, *Phys. Rev.* **D79**, 064036 (2009), arXiv:0811.2197 [hep-th].
- [26] C. Deffayet, X. Gao, D. A. Steer, and G. Zahariade, *Phys. Rev.* **D84**, 064039 (2011), arXiv:1103.3260 [hep-th].
- [27] T. Kobayashi, M. Yamaguchi, and J. Yokoyama, *Prog. Theor. Phys.* **126**, 511 (2011), arXiv:1105.5723 [hep-th].
- [28] S. Bahamonde *et al.*, *Phys. Rept.* **775-777**, 1 (2018), arXiv:1712.03107 [gr-qc].

- [29] B. Wang, E. Abdalla, F. Atrio-Barandela, and D. Pavan, *Rept. Prog. Phys.* **79**, 096901 (2016), arXiv:1603.08299 [astro-ph.CO].
- [30] N. Tamanini, *Phys. Rev.* **D92**, 043524 (2015), arXiv:1504.07397 [gr-qc].
- [31] J. D. Bekenstein, *Phys. Rev.* **D48**, 3641 (1993), arXiv:gr-qc/9211017.
- [32] L. Amendola, *Phys. Rev.* **D60**, 043501 (1999), arXiv:astro-ph/9904120.
- [33] J. Gleyzes, D. Langlois, M. Mancarella, and F. Vernizzi, *JCAP* **1508**, 054 (2015), arXiv:1504.05481 [astro-ph.CO].
- [34] C. G. Boehmer, N. Tamanini, and M. Wright, *Phys. Rev.* **D91**, 123002 (2015), arXiv:1501.06540 [gr-qc].
- [35] C. G. Boehmer, N. Tamanini, and M. Wright, *Phys. Rev.* **D91**, 123003 (2015), arXiv:1502.04030 [gr-qc].
- [36] C. Skordis, A. Pourtsidou, and E. J. Copeland, *Phys. Rev.* **D91**, 083537 (2015), arXiv:1502.07297 [astro-ph.CO].
- [37] L. Amendola, *Phys. Rev.* **D62**, 043511 (2000), arXiv:astro-ph/9908023.
- [38] A. Golovnev, V. Mukhanov, and V. Vanchurin, *JCAP* **0806**, 009 (2008), arXiv:0802.2068 [astro-ph].
- [39] C. Armendariz-Picon, *JCAP* **0407**, 007 (2004), arXiv:astro-ph/0405267.
- [40] W. Zhao, *Int. J. Mod. Phys.* **D18**, 1331 (2009), arXiv:0810.5506 [gr-qc].
- [41] T. S. Koivisto and N. J. Nunes, *Phys. Rev.* **D88**, 123512 (2013), arXiv:1212.2541 [astro-ph.CO].
- [42] T. Ngampitipan and P. Wongjun, *JCAP* **1111**, 036 (2011), arXiv:1108.0140 [hep-ph].
- [43] Y.-H. Yao, Y.-J. Yan, and X.-H. Meng, *Eur. Phys. J.* **C78**, 153 (2018), arXiv:1704.05772 [astro-ph.CO].
- [44] H. Wei and R.-G. Cai, *Phys. Rev.* **D73**, 083002 (2006), arXiv:astro-ph/0603052.
- [45] R. C. G. Landim, *Eur. Phys. J.* **C76**, 480 (2016), arXiv:1605.03550 [hep-th].
- [46] T. Koivisto and D. F. Mota, *JCAP* **0808**, 021 (2008), arXiv:0805.4229 [astro-ph].
- [47] S. Nakamura, R. Kase, and S. Tsujikawa, *JCAP* **1912**, 032 (2019), arXiv:1907.12216 [gr-qc].
- [48] G. Tasinato, *JHEP* **1404**, 067 (2014), arXiv:1402.6450 [hep-th].
- [49] L. Heisenberg, *JCAP* **1405**, 015 (2014), arXiv:1402.7026 [hep-th].
- [50] E. Allys, P. Peter, and Y. Rodriguez, *JCAP* **1602**, 004 (2016), arXiv:1511.03101 [hep-th].
- [51] E. Allys, J. P. Beltran Almeida, P. Peter, and Y. Rodriguez, *JCAP* **1609**, 026 (2016), arXiv:1605.08355 [hep-th].
- [52] J. Beltran Jimenez and L. Heisenberg, *Phys. Lett.* **B757**, 405 (2016), arXiv:1602.03410 [hep-th].
- [53] B. J. Barros, *Phys. Rev.* **D99**, 064051 (2019), arXiv:1901.03972 [gr-qc].
- [54] E. Allys, P. Peter, and Y. Rodriguez, *Phys. Rev.* **D94**, 084041 (2016), arXiv:1609.05870 [hep-th].
- [55] J. Beltran Jimenez and L. Heisenberg, *Phys. Lett.* **B770**, 16 (2017), arXiv:1610.08960 [hep-th].
- [56] V. Papadopoulos, M. Zarei, H. Firouzjahi, and S. Mukohyama, *Phys. Rev.* **D97**, 063521 (2018), arXiv:1801.00227 [hep-th].
- [57] A. E. Gumrukcuoglu and R. Namba, *Phys. Rev.* **D100**, 124064 (2019), arXiv:1907.12292 [hep-th].
- [58] A. De Felice and A. Naruko, (2019), arXiv:1911.10960 [gr-qc].
- [59] E. M. Teixeira, A. Nunes, and N. J. Nunes, *Phys. Rev.* **D100**, 043539 (2019), arXiv:1903.06028 [gr-qc].
- [60] R. Kimura, A. Naruko, and D. Yoshida, *JCAP* **1701**, 002 (2017), arXiv:1608.07066 [gr-qc].
- [61] L. Ackerman, M. R. Buckley, S. M. Carroll, and M. Kamionkowski, *Phys. Rev.* **D79**, 023519 (2009), arXiv:0810.5126 [hep-ph].
- [62] W. Fischler and J. Meyers, *Phys. Rev.* **D83**, 063520 (2011), arXiv:1011.3501 [astro-ph.CO].
- [63] M. Archidiacono, E. Calabrese, and A. Melchiorri, *Phys. Rev.* **D84**, 123008 (2011), arXiv:1109.2767 [astro-ph.CO].
- [64] J. Hasenkamp and J. Kersten, *JCAP* **1308**, 024 (2013), arXiv:1212.4160 [hep-ph].
- [65] D. Baumann, D. Green, J. Meyers, and B. Wallisch, *JCAP* **1601**, 007 (2016), arXiv:1508.06342 [astro-ph.CO].
- [66] A. Mehrabi, A. Maleknejad, and V. Kamali, *Astrophys. Space Sci.* **362**, 53 (2017), arXiv:1510.00838 [astro-ph.CO].